

J16.1 ON THE COUPLING BETWEEN URBAN SURFACE WIND FIELDS AND SKIMMING FLOW

Bruce B. Hicks, William R. Pendergrass Jr.*, Christoph A. Vogel*, and Richard S. Artz**

Metcorps
P.O. Box 1510
Norris, TN 37828

* NOAA/ARL/ATDD
P.O. Box 2456
Oak Ridge, TN 37831

** NOAA/ARL
1315 East West Highway
Silver Spring, MD 20910

1. INTRODUCTION

People in urban areas and cities are affected by a layer of the atmosphere below that which is normally forecast. While precipitation, cloud cover and insolation are appropriately forecast, the surface wind speed and even sometimes air temperature and humidity are not. The reason is clear – the air near the surface is affected by the obstacles that populate the surface, and the characteristics of these obstacles are not incorporated in current forecasting models. The critical roughness characteristics of the surface change markedly from location to location. The street canyons of New York City clearly impose different constraints on the surface boundary layer than the broad boulevards of Washington, DC. In this regard, Washington DC is an unusual and perhaps unique city. The height of buildings is constrained by the 1910 amendments of the original (1899) “Heights of Buildings” act of Congress – new buildings can be no more than 20 feet (~ 6m) higher than the width of the street on which they are situated. Spires and other similar installations are permitted on the roofs, provided they are set well back from the street frontage of the building. Washington DC is on comparatively flat land, so that the building height constraint results in a spatial homogeneity that is unusual for a major city. New York City is certainly different, with exceedingly tall buildings and considerable spatial heterogeneity even over short distances.

The present attention is on forecasting dispersion in and around cities, with potential application to managing the consequences of a release of some hazardous material into the urban atmosphere. The goal is to demonstrate how existing surface network data might be used to improve dispersion calculations in populated areas. An accompanying paper addresses the ways in which surface network data might be used to improve dispersion modeling for urban areas (Callahan and Hicks, 2008).

The surface network data are derived from the national “Weatherbug” network of AWS Convergence Technologies, Inc. (see Figure 1). In this network, anemometers are selected for their ruggedness rather

than sensitivity, with corresponding limitations on low wind speed performance. The instrumentation is typically deployed on 2 to 3 m masts attached to the edges of roofs of buildings, sometimes below the height of surrounding trees. The network is not designed to provide uniform spatial coverage but is concentrated where people live.

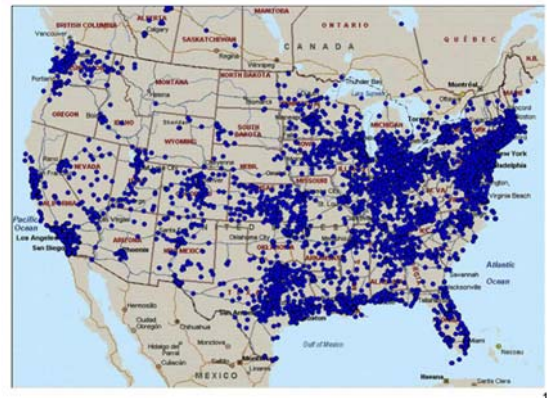


Figure 1. The national surface meteorological network of AWS Convergence Technologies, Inc.

The DCNet program employs three-dimensional sonic anemometers, erected on 10 m towers on the roofs of buildings, situated to minimize the effects of nearby obstructions. The Washington distribution of DCNet sites is shown in Figure 2. The intent of DCNet is to

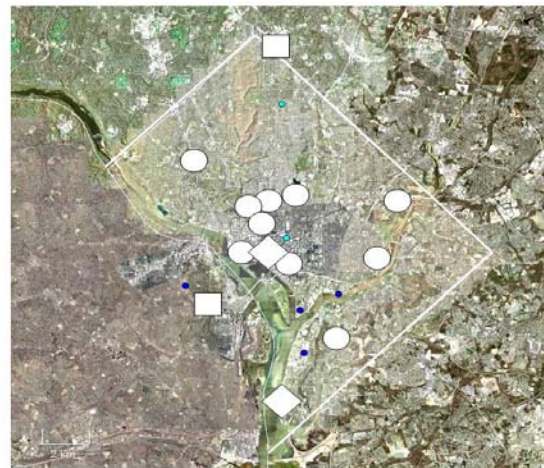


Figure 2. DCNet sites in the Washington area.

Corresponding author address: Bruce B. Hicks, Metcorps, P.O. Box 1510, Norris, TN 37828; e-mail: hicks.metcorps@gmail.com.

TABLE 1

Site details of current DCNet installations. H is the height above ground level. All towers are 10 m tall.

Washington, DC	Lat (N)	Long (W)	H
Dept. Commerce (DOC)	38.894	77.033	40 m
Nat. Acad. Sci. (NAS)	38.893	77.048	25 m
DC Municipal Ctr. (WMC)	38.917	77.033	40 m
Dept. of Energy (DOE)	38.887	77.025	40 m
Naval Res. Labs. (NRL)	38.821	77.025	30 m
Navy Annex (NAX)	38.868	77.068	30 m
NOAA, Silver Spg. (SSG)	38.992	77.030	60 m
DC Arboretum (ARB)	38.916	76.964	10 m
DC Emerg. Mgt. (EMA)	38.854	76.995	20 m
R.F.Kennedy Stad. (RFK)	38.889	76.973	45 m
Fort A. P. Hill (APH)	38.072	77.327	35 m
Nat. Educ. Assn. (NEA)	38.906	77.036	35 m
WTOP Television (WTO)	38.936	77.074	40 m
Howard University (HU)	38.922	77.021	25 m
Amer. Geophys. (AGU)	38.915	77.045	28 m
New York City			
Env. Meas. Lab. (EML)	40.726	74.008	36 m
Times Square (TSQ)	40.760	73.984	125 m

obtain micrometeorological observations to develop a better understanding of urban meteorology. For the analysis that follows, two DCNet sites will be emphasized. The first of these (SSG) is on the roof of the tallest building of the campus of the National Oceanic and Atmospheric Administration, in Silver Spring, Maryland. The second location is above the Navy Annex (NAX) of the Pentagon complex, in Virginia. Later, additional Washington DC locations will be considered. Finally, the New York City data will be examined. The New York City data are from stations on the roof of the Environmental Measurements Laboratory (EML) near Greenwich Village, and above a tall office tower adjacent to Times Square (TSQ) in central Manhattan.

2. ANALYSIS STEPS

The density of AWS stations in the areas around the Washington DCNet sites is such that there are usually 10 to 12 stations within a 5 km radius. Accordingly, the analysis that follows is based on wind data from surface stations within 5 km of the designated central DCNet sites. Data derived from both the AWS sub-networks and the DCNet sites have been arranged in parallel 15-minute sequences. Two weeks of data from October 2005 will be employed.

Because of the requirement to combine velocity data from many sources, the wind measurements have been resolved into orthogonal components, East-West (U) and North-South (V). The derivation of

network averages to compare against central DCNet data involves the following steps.

1. Derive the average velocity components across the surface network. If each station reports velocity components U and V, then the 15-minute averages for each station are $\underline{U} = (\sum U)/n$, where n is the number of values, and similarly for \underline{V} . The data set for each site also includes values of the relevant standard deviations – $\sigma(U)$ and $\sigma(V)$.
2. From the averages \underline{U} and \underline{V} for each station, we compute the subnetwork average velocity components, \underline{U} and \underline{V} . If there are N stations in the subnetwork, then $\underline{U} = (\sum U)/N$. The subnetwork vector mean speed is then computed as $\underline{u} = \sqrt{\underline{U}^2 + \underline{V}^2}$.
3. Compute the average standard deviations of the velocity components ($\sigma(U)$ and $\sigma(V)$) reported for each of the sites. The result indicates the average standard deviations in time, across the array – $\underline{\sigma(U)}$ and $\underline{\sigma(V)}$.
4. Compute the standard deviation computed from the N average velocity components (\underline{U} and \underline{V}) from individual stations (indicating the relevant standard deviation in space, across the array – $\sigma(\underline{U})$ and $\sigma(\underline{V})$).
5. From the temporal and spatial quantities of items 3 and 4, we compute the corresponding speed variables following the path of item 2:

$$\sigma_t(\text{speed}) = \sqrt{(\underline{\sigma(U)})^2 + (\underline{\sigma(V)})^2},$$

and similarly for $\sigma_s(\text{speed})$ based on the results of step 4. Note that $\sigma_t(\text{speed})$ is not the same as the conventional $\sigma(u)$, since derivation of $\sigma(u)$ from the orthogonal components $\sigma(\underline{U})$ and $\sigma(\underline{V})$ requires a coordinate rotation step for which covariance data (U and V) are required.

6. The total speed standard deviation is computed by combining the time and space products of step 5, following the path of step 2.

3. COUPLING OF VELOCITIES

Near the surface, the turbulent fluctuations that cause dispersion are due to mechanical drag of the wind on surface obstacles, convection, surface traffic, and similar factors. Instrumentation located above surface obstacles will respond to the wind field affected by the upwind area, in both its mean and fluctuating quantities. Hence, the DCNet instrumentation is intended to provide measurements indicative of some surface upwind which serves as a sink for momentum and a source of turbulent kinetic energy. If the area in question is sufficiently spatially homogeneous, then we might expect to find strong relationships between the aggregated information derived from surface instrumentation and the wind data reported by the higher elevation DCNet sensors. The present focus

on data collected within a 5 km radius of the central DCNet sites implies an assumption that the surface is homogeneous and flat across the defined area. It remains to be seen how local inhomogeneities affect the coupling.

Figure 3 shows how the surface network-averaged 15 minute winds relate to the observations of the SSG DCNet station. The upper diagrams show the relationship involving the average surface wind speeds. The lower show the dependence of the derived mean vector velocities. The diagrams to the left are for all winds, and show evidence of surface subnetwork sensor shortcomings at low wind speeds. The diagrams to the right are constrained to include only surface data for which the average surface wind speed exceeds 1 m/s; the relationships are then improved. The correlation coefficients (R) associated with the regression lines plotted support the contention that the association is strong and best for the constrained wind speeds (> 1 m/s) and for the vector mean cases. In all cases, a visually better fit would result if the relationships were forced to pass through the origin.

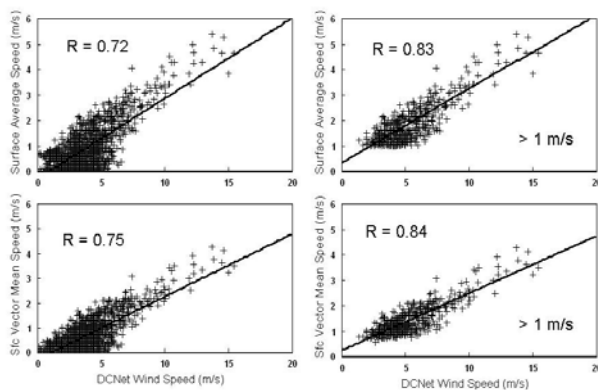


Figure 3. The relationships between AWS-station and DCNet tower velocity statistics, for the area containing Silver Spring, Maryland. The average speeds in the upper two diagrams are the linear averages of the speeds reported by each station. The vector mean speeds plotted in the lower pair of diagrams are derived by combining the averages of the U and V components reported by these same stations. Data obtained when the average surface wind speed was below 1 m/s are excluded from the right hand pair of diagrams.

The exclusion of winds below 1 m/s has two unwelcome consequences. Firstly, nighttime cases are preferentially excluded. Secondly, conditions classically characterized as “light and variable” are also excluded. Both sets of conditions are critically important to the major application considered here – the prediction of dispersion affecting people. This shortcoming can only be overcome by the use of more sensitive instrumentation, with the associated suspicion that more analysis might then be required.

Examination of data from other DCNet sites and their surrounding surface subnetworks shows that the average ratio (F_u) of surface average/DCNet wind speeds is 0.32 ± 0.11 . The two New York sites yield similar results -- the low-level EML case and the much higher elevation TSQ case (see Table 1) yield similar ratios, with averages $F_u = 0.40$ and 0.39 respectively. In these computations, data with average wind speeds below 1 m/s have been excluded. Slightly different averages result when the low wind speed cases are included in the analysis.

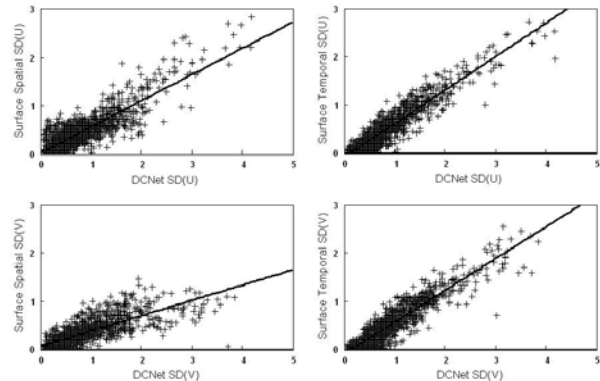


Figure 4. The relationships between spatial and temporal components of turbulence measured by the surface network and the turbulence reported by the central DCNet station, for SSG. All properties are plotted as standard deviations. Surface data are extracted from all surface reporting sites within a 5 km radius of the central DCNet station.

4. COUPLING OF TURBULENCE

Figure 4 illustrates the relationships between computed surface network spatial and temporal variances of velocity turbulence compared to the turbulence measured at the Silver Spring DCNet site. As illustrated by regression lines, it is evident that there are again strong relationships involved, but it is also clear that the dependencies are stronger than is evident in Figure 3. The corresponding correlation coefficients and slopes are as indicated, and are summarized in Table 2. In Figure 4, there is less visible evidence of a low wind speed limitation than in the case of the wind speeds themselves. Analysis of the NAX data reveals a similar set of diagrams (see Figure 5), differing mainly as a result of the obvious fact that the NAX DCNet data are obtained closer to the measurement level of the AWS data. Figure 6 is an example of how the total (spatial plus temporal) speed standard deviation derived from the surface network relates to the standard deviation of wind speed derived from coordinate rotation of the U and V data from the central DCNet tower. This example is for Silver Spring. There are two diagrams shown – the upper illustrating the relationship for all winds, the lower for the DCNet subset with average surface wind

TABLE 2

Coefficients of regression relationships derived from analysis of SSG and NAX data, and of surface data collected within a 5 km radius of these two DCNet sites. “SD” refers to a standard deviation. Values in parentheses relate to a smaller data set, for average surface wind speeds > 1 m/s. The regressions are of the form $Y = a + b.x$.

Y	x	R ²	b	a
<u>Silver Spring</u>				
Spatial SD(U)	DCNet SD(U)	0.73 (0.37)	0.54 (0.49)	0.03 (0.37)
Temporal SD(U)	DCNet SD(U)	0.87 (0.34)	0.70 (0.42)	-0.08 (0.40)
Spatial SD(V)	DCNet SD(V)	0.59 (0.31)	0.32 (0.27)	0.07 (0.25)
Temporal SD(V)	DCNet SD(V)	0.86 (0.41)	0.66 (0.44)	-0.09 (0.37)
Spatial SD(speed)	DCNet SD(speed)	0.81 (0.44)	0.45 (0.40)	0.07 (0.45)
Temporal SD(speed)	DCNet SD(speed)	0.89 (0.36)	0.70 (0.43)	-0.15 (0.54)
TOTAL SD(speed)	DCNet SD(speed)	0.88 (0.43)	0.82 (0.59)	-0.05 (0.70)
TOTAL SD(speed)	DCNet speed	0.50 (0.27)	0.27 (0.18)	-0.09 (0.82)
DCNet SD(speed)	DCNet speed	0.52 (0.71)	0.31 (0.33)	-0.00 (0.09)
<u>Navy Annex</u>				
Spatial SD(U)	DCNet SD(U)	0.67 (0.39)	0.55 (0.36)	0.05 (0.40)
Temporal SD(U)	DCNet SD(U)	0.86 (0.81)	0.63 (0.55)	-0.06 (0.12)
Spatial SD(V)	DCNet SD(V)	0.71 (0.54)	0.60 (0.54)	0.11 (0.23)
Temporal SD(V)	DCNet SD(V)	0.83 (0.70)	0.61 (0.48)	-0.02 (0.24)
Spatial SD(speed)	DCNet SD(speed)	0.81 (0.67)	0.60 (0.49)	0.10 (0.39)
Temporal SD(speed)	DCNet SD(speed)	0.87 (0.80)	0.64 (0.54)	-0.07 (0.20)
TOTAL SD(speed)	DCNet SD(speed)	0.85 (0.76)	0.87 (0.73)	0.03 (0.43)
TOTAL SD(speed)	DCNet speed	0.82 (0.80)	0.39 (0.32)	0.05 (0.41)
DCNet SD(speed)	DCNet speed	0.77 (0.74)	0.40 (0.38)	0.13 (0.35)

speeds above 1 m/s. The purpose of this figure is two-fold: first to illustrate the importance of the low wind speed limitation on the surface network data, and second to illustrate that the standard deviation of the coordinate-rotated wind speed is not the same as the vector sum of the orthogonal components as is used in other diagrams of this presentation. In common with earlier figures, the lines represent the results of linear regressions with coefficients as shown. There is little difference in the correlation coefficients, nor in the slopes (one of which is strikingly close to unity, probably fortuitously but strongly indicative of how well the data agree).

Table 2 reveals that the correlation between the standard deviation of the wind across the surface network and the DCNet observations increases with the number of surface wind components considered. The highest correlations are found for the cases in which all of the surface network quantities are combined – the total standard deviation derived by

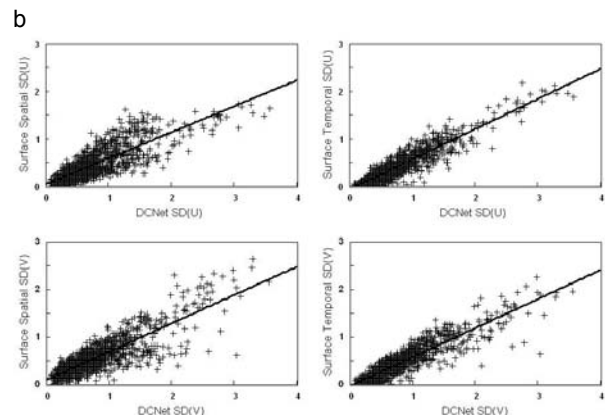


Figure 5. As for Figure 4, but for the Navy Annex site (NAX).

summing the U and V variances for the surface array is strongly correlated with the total wind standard deviation (obtained in the same way) reported by the completely independent DCNet single-tower system with a correlation coefficient of 0.94 (0.66 for $u > 1$ m/s) for SSG and 0.92 (0.87) for NAX. As expected, the slopes (“b”) associated with the NAX regressions are mostly greater than those for the SSG – the NAX DCNet measurement location is much lower than the SSG system, and its velocities are correspondingly closer to those of the surface network.

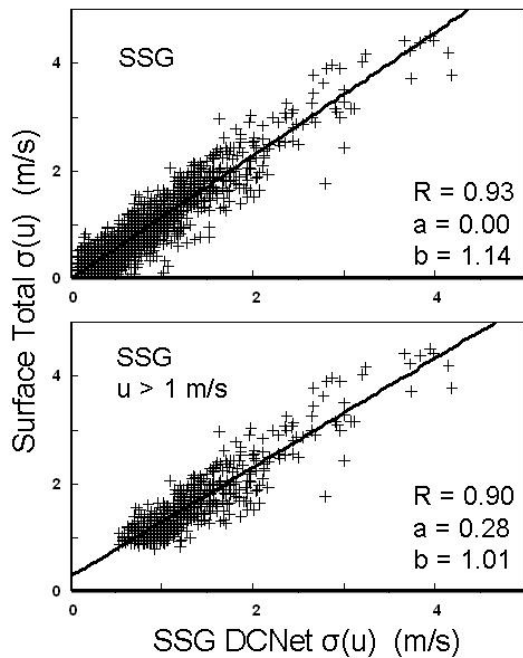


Figure 6. As for Figure 4, but for the total surface wind standard deviation derived by combining spatial and temporal terms, plotted against the central (DCNet) wind standard deviation derived by coordinate rotation.

The analysis above is certainly influenced by the resolution and sensitivity characteristics of the anemometers used in the surface arrays and in DCNet. It must be remembered that any results of the kind presented here must necessarily be influenced by the mismatching of sensors. It is concluded from these considerations that the aggregation of data from the surface subnetwork yields results that are well associated with the DCNet data, at 10 m height above rooftops, both in mean quantities and in turbulence intensities, provided the winds are strong enough for the surface network instrumentation to report accurately.

It is also informative to consider the way in which the surface wind variance is apportioned between temporal and spatial components. Figure 7 depicts the diurnal variations of the space/time ratios of the total wind component standard deviations (the left diagrams) and the ratio of the surface total wind

standard deviation to the total wind component standard deviation derived from the data of the central DCNet tower, for the two sites. There appears to be a consistent behavior, with far better ordered ratios during daytime than for night. The scatter at night appears to be associated with the low speed performance limitations of the surface anemometers. Figure 8 parallels Figure 7, but for average wind speeds > 1 m/s. It is concluded that the low speed sensor inadequacies could account for most of the apparent diurnal cycle evident in Figure 7.

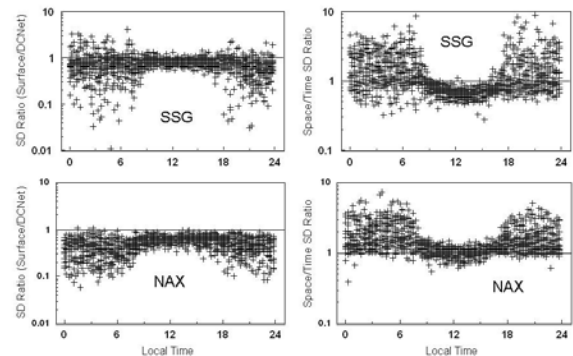


Figure 7. Two characterizations of the total surface velocity standard deviations, for the SSG and NAX sites. On the left are ratios of the total velocity component standard deviation derived from the surface array to the contemporary total component velocity standard deviation yielded by the central DCNet instrumentation. On the right are the ratios Space/Time of the velocity components derived from the surface array alone.

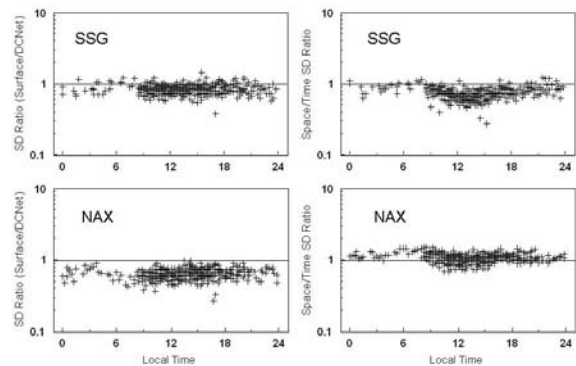


Figure 8. As in Figure 7, but after excluding all data for which the average surface wind speed was less than 1 m/s.

5. DISCUSSION AND CONCLUSIONS

It is often argued that the meteorological information content of poorly sited surface data is small, because the data are not considered representative of the grid-cells used in conventional numerical models. If the intent is to take forecasts to where they directly affect people, then we must learn how to make best use of

the many data sources already available, yielding information on the actual air affecting people. The fact that these data are not of great use in improving mesoscale meteorological models does not negate their potential utility for forecasting on a more local scale. The surface networks sample the complexity of the surface regime, whereas the rooftop systems sample the consequences of this complexity.

The wind speeds yielded by the surface-level anemometry are well correlated with the wind measured by DCNet stations at rooftop level, although not as well correlated as for the velocity variances. The average ratio of surface mean speed to DCNet rooftop speed is 32% (+/- 11%) for the Washington situations considered here, and 40% for the two New York stations (independently yielding 40% and 39%). This is in accord with the summation presented by Hanna et al. (2006), who conclude that "The mean wind speed at street level is about 1/3 of the mean wind speed at the tops of tall downtown buildings." For the purposes of operational application, a transport velocity in the surface roughness layer of 30% to 40% of the wind speed aloft appears to be appropriate for the two cities considered here.

Spatial and temporal components of the surface turbulent kinetic energy contribute approximately equally to the total turbulence intensity measured aloft. The high correlations associated with the wind variability statistics support the expectation that surface anemometry can indeed contribute to the improvement of dispersion calculations for the surface boundary layer. Wind speed and velocity component relationships are far more influenced by local surface inhomogeneities than are those for the turbulence intensity. This is in accord with the pragmatic and operational observation that turbulent kinetic energy has a far longer "memory" than does the average velocity field.

The present conclusions are influenced by the limited performance of the surface network anemometers. Better results are obtained when data with winds below 1 m/s are excluded, but this then excludes light and variable winds and preferentially affects nighttime conditions. Both of these situations are important in the context of plume dispersion. To remove this limitation, there is no option but to use anemometry with better starting speed performance (both for speed and direction). Nevertheless, it is clear that the results obtained here suggest the potential use of surface network data in modified plume dispersion models.

While, some of the instruments used to derive the present results are exposed in situations conventionally deemed unacceptable, even poorly exposed instruments can accurately report on the conditions they experience, and these conditions are indisputably part of the total atmospheric environment

under consideration. By considering an ensemble of such instruments, the analysis above shows that meaningful information can be derived for the city and surroundings of Washington, DC, and perhaps to a smaller extent to the island of Manhattan.

ACKNOWLEDGEMENTS

Several staff members of the NOAA Air Resources Laboratory assisted with the analyses presented here. Specific mention should be made of the contributions by Ron Dobosy and Ed Dumas of ARL Oak Ridge, and of Roland Draxler of ARL Silver Spring. The surface data used here were provided through a Memorandum of Understanding between NOAA and AWS Convergence Technologies, Inc., of Germantown, Maryland. Specific mention of AWS and its capabilities should not be construed as an endorsement or an indication of preference relative to other similar providers of meteorological data.

REFERENCES

- Britter, R. E., and S. R. Hanna, 2003: Flow and dispersion in urban areas. *Annu. Rev. Fluid Mech.*, **35**, 469 – 496.
- Callahan, W., and B. B. Hicks, 2008: Utilizing Surface Data in Urban Dispersion Models. Paper J16.3, this conference.
- Hanna, S. R., J. White, Y. Zhou and A. Kosheleva, 2006: Analysis of Joint Urban 2003 (JU2003) and Madison Square Garden 2005 (MSG05) Meteorological and Tracer Data. Paper J7.1 of the Sixth AMS Conference on the Urban Environment, Atlanta, GA, available at http://ams.confex.com/ams/Annual2006/techprogram/paper_104131.htm.
- Oke, T. R., 1987: *Boundary Layer Climates*. Methuen, London, U.K.